Acta Crystallographica Section B
Structural Science
ISSN 0108-7681

Electron density and electrostatic properties of two peptide molecules: tyrosyl-glycyl-glycine monohydrate and glycyl-aspartic acid dihydrate

Virginie Pichon-Pesme, Hassane Lachekar, Mohamed Souhassou and Claude Lecomte*

LCM3B, Laboratoire de Cristallographie et Modélisation des Matériaux Minéraux et Biologiques, Université Henri Poincaré-Nancy 1, UPRESA CNRS 7036, Faculté de Sciences, BP 239, 54506 Vandoeuvre les Nancy CEDEX, France

Correspondence e-mail: lecomte@lcm3b.u-nancy.fr

Received 7 December 1999
Accepted 21 March 2000

The electron density and electrostatic properties of Tyr-Gly-Gly and Gly-Asp molecules have been determined from high-resolution X-ray diffraction data at 123 K. Topological properties of the charge distribution are discussed and compared with those derived from other experimental studies on peptide molecules, and the characteristics of the (3,−1) critical points of the C═O, C—N, C—C bonds are analysed. Crystal data for Tyr-Gly-Gly: $C_{13}H_{17}N_3O_5{\cdot}H_2O$, M_r = 313, orthorhombic, $P2_12_12_1$, Z = 4, T = 123 ± 2 K; lattice parameters: a = 7.984 (2), b = 9.535 (3), c = 18.352 (5) Å, V = 1397.1 (6) Å^3, D_x = 1.49 g cm^{-3}, μ = 1.2 cm^{-1} for λ_{Mo} = 0.7107 Å. Crystal data for Gly-Asp: $C_6H_{10}N_2O_5{\cdot}2H_2O$, M_r = 212, orthorhombic, $P2_12_12_1$, Z = 4, T = 123 ± 2 K; lattice parameters: a = 9.659 (1), b = 9.672 (1), c = 10.739 (1) Å, V = 1003.3 (4) Å^3, D_x = 1.40 g cm^{-3}, μ = 1.3 cm^{-1} for λ_{Mo} = 0.7107 Å.

1. Introduction

The electron density of the title compounds has been determined to complete our database of peptides and amino acid electron-density parameters (Pichon-Pesme *et al.*, 1995). The ultimate goal of this database is to extract some universal charge-density parameters of peptides (net charges, average aspherical density parameters *etc.*) and to use the corresponding scattering factors in the structure refinement of larger biological molecules, such as proteins (Jelsch *et al.*, 1998, 2000).

In this paper we report on the analysis of the electron density and electrostatic properties of tyrosyl-glycyl-glycine monohydrate (YGG) and glycyl-L-aspartic acid dihydrate (GD). Topological characteristics of the experimental electron density are also discussed, together with those of other peptide molecules. Fig. 1 shows an *ORTEP* view of these two compounds.

2. Experimental

2.1. Data collection

The tripeptide YGG was crystallized by slow evaporation from 50% acetic solution containing 10 mg ml^{-1} of tripeptide equilibrated *via* the vapour phase against absolute 2-propanol. The dipeptide GD was crystallized by slow evaporation from 30% ethanol solution containing 10 mg ml^{-1} of dipeptide.

Single crystals (0.30 × 0.26 × 0.20 mm for YGG and 0.24 × 0.30 × 0.40 mm for GD) were used to measure low-temperature Mo $K\alpha$ X-ray diffraction data on a Nonius CAD-4F diffractometer equipped with a nitrogen gas stream appa-

ratus and installed in a dry-box to prevent ice formation on the crystal. The gas stream temperature was maintained at 123 ± 2 K. The temperature was calibrated using the para-ferroelectric KDP phase transition (T_c = 123 K). Lattice parameters were obtained by least-squares fit to the optimized setting angles of 25 reflections with $12 < 2\theta < 21°$. Intensity data were recorded in the same way for both compounds. In the following, we first will give the experimental parameters of YGG and those corresponding to GD will be given in brackets. Intensities were measured to a resolution of 1.32 Å^{-1} for a total of 18 847 reflections [1.20 Å^{-1} for 14 895 reflections] in the ω–2θ scan mode. For $\sin\theta/\lambda < 0.95$ Å^{-1} [0.90 Å^{-1}] three symmetry-equivalent reflections were collected. During the data collection a first refinement of the structure was performed and intensities with $0.95 < \sin\theta/\lambda < 1.32$ Å^{-1} [$0.90 < \sin\theta/\lambda < 1.20$ Å^{-1}] were calculated: among these reflections only the significant reflections with [$I > I_{ref} * 0.25$] were measured (two symmetry equivalents), where I_{ref} correspond to I(0, 4, 15) [I(15, 6, 2)]. The total scan ($\Delta\omega$) was $0.9 + 0.35\tan\theta°$ [$0.8 + 0.35\tan\theta°$] with a constant detector aperture of 6 × 4 mm^2. A prescan speed $v = d\omega/dt$ of 2.75° min^{-1} and a final scan speed depending on the signal-to-noise ratio ($0.74 < v < 2.75°$ min^{-1}) were used for the low-angle data collection. The high-angle data were measured at a constant scan speed (0.66° min^{-1} [0.92° min^{-1}]). During the data collection five standard reflections were measured at 2 h intervals. The total exposure time was 698 (366) h. During both experiments, no problems associated with the crystals, temperature or diffractometer occurred.

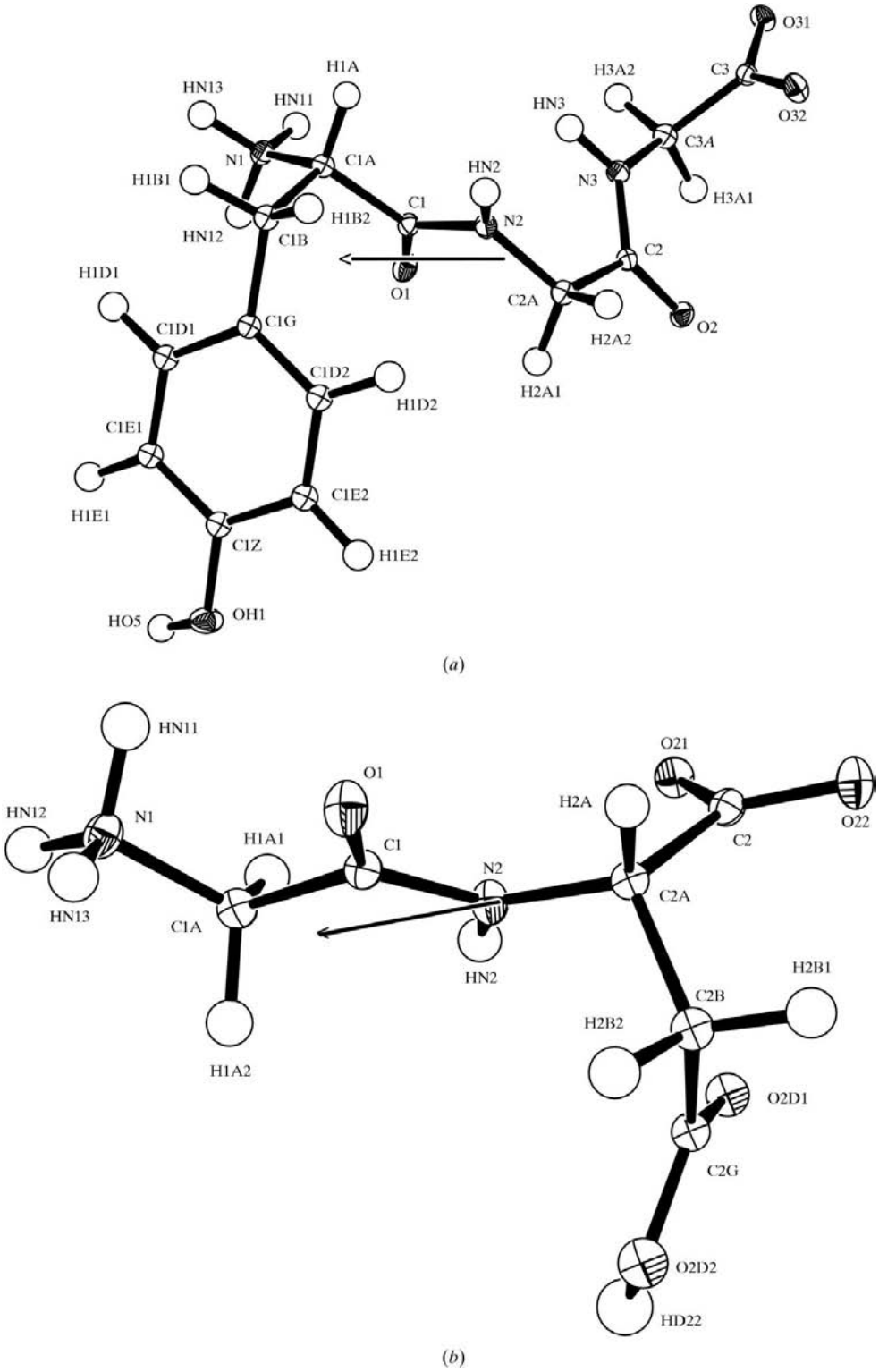

Figure 1
*ORTEP*III (Burnett & Johnson, 1996) view of (*a*) YGG and (*b*) GD. The arrow represents the direction of the calculated dipole moment of the peptide molecule.

2.2. Data processing

Data reduction and error analysis were performed using *DREAR* programs (Blessing, 1987, 1989). Reflection integration limits were taken from a Lorentzian model of the peak-width variations. A polynomial fit to the variation of the standard reflections intensities over the X-ray exposure time was used to scale the data and to derive the

Table 1
Least-squares statistics-of-fit for different refinements.

$s = \sin\theta/\lambda$; $R = \Sigma\,(|F_o| - K|F_c|)/\Sigma|F_o|$; $wR = (\chi^2/\Sigma w|F_o|^2)^{1/2}$; $\chi^2 = \Sigma w(|F_o| - K|F_c|)^2$; $w = \sigma^{-2}(|F_o|)$; g.o.f. = $[\chi^2/(n - m)]^{1/2}$; n: data; m: parameters; K: scale factor.

	s (Å^{-1})	n_o	n_v	R	wR	g.o.f.
YGG						
Spherical A	$s > 0.80$	1965	199	0.0717	0.0663	0.98
Spherical B	$s < 0.80$	2801	77	0.0486	0.0486	3.02
Multipolar C	$s < 1.15$	4766	412	0.0356	0.0209	1.02
Multipolar D	$s < 1.15$	4766	551	0.0345	0.0202	0.99
Kappa E	$s < 1.15$	4766	85	0.0461	0.0388	1.86
GD						
Spherical A	$s > 0.90$	1253	136	0.0505	0.0547	0.94
Spherical B	$s < 0.90$	2862	57	0.0391	0.0473	1.99
Multipolar C	$s < 1.20$	4115	344	0.0262	0.0273	0.99
Multipolar D	$s < 1.20$	4115	456	0.0249	0.0261	0.96
Kappa E	$s < 1.20$	4115	47	0.0351	0.0409	1.47

instrumental instability coefficient $\langle p\rangle$ = 0.0095 (0.027; McCandlisch *et al.*, 1975) used for the calculation of

$$\sigma^2(F^2) = \sigma_c^2(F^2) + (\langle p\rangle F^2)^2,$$

with $\sigma_c{}^2$ being the estimated error from the calculation of the propagation of errors, in which counting statistics and scan-angle setting uncertainties [$\sigma(\omega) = 0.005^\circ$] made the most important conditions. The 18 847 (14 895) reflections with $\sin\theta/\lambda < 1.32$ Å^{-1} (1.20 Å^{-1}) were symmetry-averaged to end up with 5849 (4775) unique data ($I > 0$; $\sin\theta/\lambda < 1.15$ Å^{-1} [1.20 Å^{-1}]), of which 4766 (4115) had $I > 2\sigma(I)$ [$3\sigma(I)$]. Internal agreements as calculated in *DREAR* (Blessing, 1987, 1989) are $R(F^2) = 0.018$ (0.040) and $wR(F^2) = 0.031$ (0.041) for all data and $R(F^2) = 0.018$ (0.040) and $wR(F^2) = 0.013$ (0.022) for 874 (630) unique data with $\sin\theta/\lambda < 0.5$ Å^{-1}.

2.3. Least-squares refinements

The xyz, U^{ij} atomic parameters were determined using the *SHELXS* program (Sheldrick, 1990); they are in good agreement with those given by Carson & Hackert (1978) for YGG and by Eggleston & Hodgson (1982) for GD. All H atoms for both molecules were found in difference-Fourier syntheses.

A spherical-atom refinement using high-order data ($\sin\theta/\lambda > 0.8$ Å^{-1} for YGG and $\sin\theta/\lambda > 0.9$ Å^{-1} for GD) was carried out to better estimate the atomic positional and thermal parameters of non-H atoms (refinement A). Then only hydrogen atomic parameters (xyz, $U_{\rm iso}$) were refined with low-order data ($\sin\theta/\lambda < 0.8$ Å^{-1} for YGG and $\sin\theta/\lambda < 0.9$ Å^{-1} for GD; refinement B). The coordinates of the H atoms were then adjusted by extending along the Csp^3—H, Csp^2—H, N—H and O—H distances, respectively, to 1.085, 1.076, 1.032 and 0.964 Å, which are equal to the average values from neutron diffraction (Allen, 1986). These parameters were kept fixed during all the following calculations. The good quality of these spherical atom refinements is shown in Table 1. The high value of the goodness-of-fit (3.02 for YGG, 1.99 for GD) shows that the spherical atom model is not precise enough to describe the valence bond density and that a better electron density model is necessary. Therefore, the multipolar electron density model of Hansen & Coppens (1978) (program *MOLLY*) was used to analyse the charge density $\rho(\mathbf{r})$

$$\rho(\mathbf{r}) = \rho_{\rm core}(r) + \kappa^3 P_{\rm val}\rho(\kappa r) + \sum_{l=1}^{3}\kappa'^3 R_l(\kappa' r)\sum_{m=0}^{l} P_{lm\pm} y_{lm\pm}(\theta,\varphi), \qquad (1)$$

where

$$R_l(r) = N_l r^{n} \exp(-\xi r).$$

The multipole order was limited to $l = 3$ (octopole) for non-H atoms and to $l = 1$ (dipole) for H atoms. In order to store the P_{lm} parameters in our peptide database (Pichon-Pesme *et al.*, 1995), the local coordinate system in which the P_{lm} are calculated and the n and ξ parameters of the radial functions were chosen to be identical to those defined in our previous studies on peptide molecules (Souhassou *et al.*, 1991, 1992; Wiest *et al.*, 1994; Pichon-Pesme *et al.*, 1992; Espinosa *et al.*, 1996; Pichon-Pesme & Lecomte, 1998; Dahaoui *et al.*, 1999; Benabicha *et al.*, 2000). The bound atom form factor for H atoms from Stewart *et al.* (1965), the form factor for the non-H atoms calculated from Clementi & Raimondi (1963) wavefunctions, and the real and imaginary dispersion corrections to the form factors given by Cromer (1974) were used in the structure-factor calculations.

At the beginning of the multipole refinement, several constraints (chemical type and site symmetry) were applied to reduce the number of variables and to stabilize the refinement. Each aromatic ring atom was assumed to have 2*mm* local symmetry; the peptide bond atoms and those of carboxyl groups were constrained to be planar. No symmetry constraint was imposed to Csp^3 atoms. Then, because no problem occurred during the refinements (refinement C, Table 1), all chemical constraints were suppressed for the GD molecule. For YGG the five C atoms of the tyrosine ring which are not bound to the OH group were kept identical. No local symmetry was assigned to the GD water molecules, whereas a mirror symmetry was imposed to the YGG water molecules. Concerning the H atoms, only one dipole along the X—H bond was used to describe the bonding density. To keep the electroneutrality of each molecule, the P_v parameters of the atoms belonging to the peptide molecules and those of the water molecules in the asymmetric unit were refined separately. Then no charge transfer was allowed. No extinction parameter refinement was deemed necessary. The total number of parameters was 551 (YGG) and 456 (GD), and these parameters were refined against 4766 reflections [$I > 2\sigma(I)$] for YGG and against 4115 reflections for GD [$I > 2\sigma(I)$, refinement D]. For refinements C and D, the strategy was the following: first the electron density parameters were refined, then the atomic positional and thermal parameters. This process was recycled until convergence.

Finally, a kappa refinement (E; Coppens *et al.*, 1979) was also carried out to estimate the net charges of the atoms. The statistical figures of merit for the different refinements are given in Table 1. Residual density calculated on both mole-

cules after refinement D did not reveal density peaks greater than 0.10 e Å^{-3} (see supplementary material).[1] The kappa net charges are given in Table 2. The atomic coordinates, main bond lengths, angles and hydrogen-bond geometry based on the last multipole refinement (D) are listed in Tables 2–4. The anisotropic mean-square thermal displacement parameters, torsion angles, multipole parameters and a list of structure factors are given as supplementary material.

3. Results and discussion

3.1. Deformation electron densities

In order to reveal the quality of data, experimental deformation density maps (see, for example, Pichon-Pesme & Lecomte, 1998, for definition) were calculated in all atomic groups of both molecules. For each map only reflections with $\sin\theta/\lambda$ less than 0.9 Å^{-1} were included, because additional high-order reflections do not carry much information regarding valence charge density (see, for example, Jelsch *et al.*, 1998) and increase the noise level. These maps exhibit the general features already observed in our previous studies of peptide electron density. The average peak height in the C—C bond of the tyrosine group reaches 0.55 e Å^{-3} in YGG compared with 0.53 e Å^{-3} in Leu-enkephalin (Wiest *et al.*, 1994) and the corresponding peak height for the C—O bond of tyrosine reaches 0.35 and 0.25 e Å^{-3}, respectively. All peptide bonds (CONH) have similar charge density (Fig. 2*a*); in YGG the lone-pair density of the carbonyl O2 atom is slightly asymmetric owing to hydrogen bonding (Fig. 2*b*). The higher lone-pair peak corresponds to the shorter H···O distance (H*w*2—O2 = 1.791 Å compared with HN13—O2 = 1.926 Å); furthermore, in the shortest hydrogen bond, oxygen, hydrogen and donor atoms are aligned leading to a maximal interaction (O2—H*w*2—O6 = 175.7°).

3.2. Electrostatic properties

The electrostatic potential was calculated for each molecule considered as a pseudo-isolated entity removed from the crystal lattice using *ELECTROS* (Ghermani *et al.*, 1992). Fig. 3(*a*) shows the electrostatic potential generated by YGG in the $N_3C_2O_2$ peptide plane. There is, as expected, a negative region around the O2 atom (V_{min} = −0.33 e Å^{-1} corresponding to an electrostatic energy of 458 kJ mol^{-1} for a unit test charge). Fig. 3(*b*) compares the potential obtained in the same plane from a cluster of two YGG molecules and one water, which interact in the crystal *via* hydrogen bonds. Positive valleys are present between acceptor and H atoms, as previously observed for example in *N*-acetyl-$\alpha\beta$-dehydrophenylalanine methylamide (Lecomte *et al.* 1992), cytidine (Chen & Craven, 1995) and glycyl-L-threonine dihydrate (Benabicha *et al.*, 2000).

The electrostatic potential calculated in the carboxyl plane of YGG shows an extensive electronegative region around both O atoms (Fig. 4*a*). This is the result of superposing regions of negative potential owing to the two O atoms with high negative net charges [O31 = −0.42 (2) e; O32 = −0.33 (1) e]. Each carboxyl O atom interacts *via* two short hydrogen bonds (Table 4) and the resulting electrostatic potential calculated from a cluster of four YGG molecules and one water is shown in Fig. 4(*b*). This very negative potential is

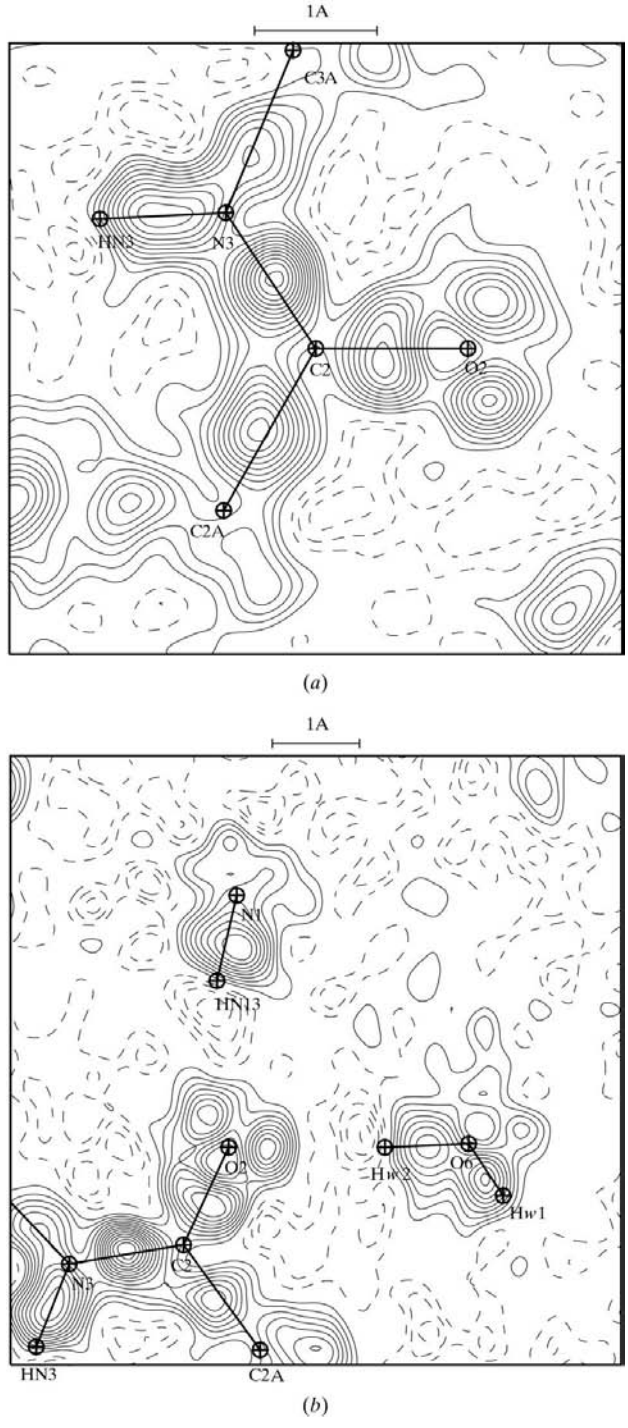

Figure 2
Experimental deformation electron density in YGG (*a*) the peptide bond plane and (*b*) the O6—O2—N1 plane. Contour interval 0.05 e Å^{-3}; positive solid line, negative dashed line, zero contour omitted.

[1] Supplementary data for this paper are available from the IUCr electronic archives (Reference: BS0010). Services for accessing these data are described at the back of the journal.

Table 2
Fractional coordinates, equivalent displacement parameters and net charges after refinement D.

U_{eq} is defined as one third of the trace of the orthogonalized U^{ij} tensor.

	x	*y*	*z*	U_{eq}	Net charge
(*a*) YGG					
O1	0.29679 (6)	0.38515 (6)	−0.05665 (3)	0.015 (1)	−0.32
O2	0.14819 (7)	0.49680 (6)	0.14781 (2)	0.014 (1)	−0.39
O31	0.21920 (6)	0.99642 (5)	0.11764 (3)	0.014 (1)	−0.54
O32	−0.00356 (7)	0.85722 (5)	0.13385 (3)	0.015 (1)	−0.54
OH1	0.22461 (7)	−0.22641 (5)	−0.08568 (3)	0.019 (1)	−0.50
O6	0.07754 (7)	0.22615 (5)	0.18999 (3)	0.016 (1)	−0.50
N1	0.30502 (7)	0.43883 (6)	−0.19877 (3)	0.012 (1)	−0.67
N2	0.02553 (7)	0.44865 (6)	−0.04149 (3)	0.011 (1)	−0.66
N3	0.15617 (8)	0.64654 (6)	0.05190 (3)	0.013 (1)	−0.52
C1	0.16215 (9)	0.42107 (7)	−0.08231 (3)	0.010 (1)	+0.23
C1A	0.13657 (9)	0.43357 (7)	−0.16456 (3)	0.011 (1)	−0.08
C1B	0.03320 (9)	0.30932 (7)	−0.19391 (4)	0.012 (1)	−0.38
C2	0.11734 (8)	0.52464 (7)	0.08310 (4)	0.011 (1)	+0.12
C2A	0.02899 (9)	0.41640 (7)	0.03566 (3)	0.012 (1)	−0.20
C3A	0.24986 (9)	0.75644 (7)	0.08749 (4)	0.014 (1)	−0.13
C3	0.14502 (9)	0.88070 (7)	0.11413 (3)	0.011 (1)	+0.38
C1G	0.08635 (9)	0.16721 (7)	−0.16566 (4)	0.011 (1)	−0.11
C1E1	0.25135 (9)	−0.04652 (7)	−0.17721 (4)	0.013 (1)	−0.11
C1D1	0.20376 (9)	0.08535 (7)	−0.20273 (3)	0.013 (1)	−0.11
C1Z	0.18290 (9)	−0.09706 (7)	−0.11268 (4)	0.013 (1)	+0.11
C1D2	0.01886 (9)	0.11386 (7)	−0.10092 (4)	0.013 (1)	−0.11
C1E2	0.06705 (9)	−0.01667 (8)	−0.07405 (4)	0.013 (1)	−0.11
H1A	0.07006	0.52955	−0.17707	0.014 (4)	+0.24
H1B1	0.04423	0.31095	−0.25288	0.016 (4)	+0.24
H1B2	−0.09621	0.32677	−0.17925	0.016 (4)	+0.24
H2A1	0.09148	0.31784	0.04781	0.016 (4)	+0.24
H2A2	−0.09968	0.40770	0.05397	0.016 (4)	+0.24
H3A1	0.30966	0.71877	0.13672	0.018 (4)	+0.24
H3A2	0.34161	0.79795	0.04932	0.018 (4)	+0.24
HN11	0.38315	0.51581	−0.17837	0.016 (4)	+0.35
HN12	0.37513	0.34997	−0.18861	0.016 (4)	+0.45
HN13	0.29803	0.44493	−0.25472	0.016 (4)	+0.35
HN2	−0.08852	0.46827	−0.06568	0.016 (4)	+0.28
HN3	0.13114	0.66368	−0.00231	0.016 (4)	+0.32
H1D1	0.25965	0.12356	−0.25196	0.017 (4)	+0.17
H1E1	0.34288	−0.10783	−0.20536	0.017 (4)	+0.17
H1D2	−0.06714	0.17524	−0.06934	0.017 (4)	+0.17
H1E2	0.02153	−0.05945	−0.02374	0.017 (4)	+0.17
HO5	0.32902	−0.26132	−0.10473	0.015 (4)	+0.30
H*w*1	0.12995	0.15704	0.15916	0.021 (5)	+0.26
H*w*2	0.10614	0.31906	0.17356	0.021 (5)	+0.40
(*b*) GD					
O21	−0.78621 (4)	−0.27464 (4)	−0.22757 (4)	0.015 (1)	−0.28
O22	−0.94748 (4)	−0.14220 (4)	−0.31605 (4)	0.017 (1)	−0.29
C2	−0.82426 (5)	−0.16995 (5)	−0.28803 (5)	0.012 (1)	+0.26
C2A	−0.71303 (5)	−0.06645 (5)	−0.32942 (5)	0.013 (1)	+0.00
N2	−0.57674 (4)	−0.11497 (4)	−0.29271 (5)	0.014 (1)	−0.40
C1	−0.48454 (5)	−0.03277 (5)	−0.23657 (4)	0.012 (1)	+0.27
O1	−0.50751 (4)	0.08792 (4)	−0.20603 (4)	0.018 (1)	−0.34
C1A	−0.34498 (5)	−0.10086 (5)	−0.21273 (5)	0.015 (1)	−0.36
N1	−0.26556 (5)	−0.01730 (5)	−0.12333 (5)	0.015 (1)	−0.63
C2B	−0.71587 (6)	−0.03553 (5)	−0.46976 (5)	0.016 (1)	−0.44
C2G	−0.67069 (5)	−0.16118 (5)	−0.54215 (5)	0.014 (1)	+0.10
O2D1	−0.71240 (5)	−0.27664 (4)	−0.51789 (4)	0.019 (1)	−0.22
O2D2	−0.58222 (5)	−0.13440 (4)	−0.63233 (5)	0.022 (1)	−0.31
O*w*1	−0.95007 (4)	−0.41590 (4)	−0.06995 (4)	0.018 (1)	−0.31
O*w*2	−0.39866 (5)	0.19248 (5)	−0.48429 (5)	0.024 (1)	−0.31
H2A	−0.74147 (3)	0.02974 (3)	−0.28281 (3)	0.016 (6)	+0.10
HN2	−0.54291 (3)	−0.21517 (3)	−0.30427 (3)	0.019 (6)	+0.44
H1A1	−0.36615 (3)	−0.20362 (3)	−0.17549 (3)	0.020 (6)	+0.17
H1A2	−0.29585 (3)	−0.10799 (3)	−0.30204 (3)	0.020 (7)	+0.00
HN11	−0.32591 (3)	−0.00694 (3)	−0.04364 (3)	0.020 (7)	+0.43
HN12	−0.17890 (3)	−0.07177 (3)	−0.09329 (3)	0.020 (6)	+0.43
HN13	−0.24809 (3)	0.07590 (3)	−0.16559 (3)	0.020 (6)	+0.43
H2B1	−0.82348 (3)	−0.02143 (3)	−0.49598 (3)	0.021 (7)	+0.21
H2B2	−0.64005 (3)	0.04544 (3)	−0.48652 (3)	0.021 (6)	+0.21
HD22	−0.54140 (4)	−0.21932 (4)	−0.66273 (3)	0.030 (8)	+0.27
H*w*11	−0.89563 (3)	−0.36954 (3)	−0.13191 (3)	0.024 (7)	+0.03
H*w*12	−1.00414 (3)	−0.48600 (3)	−0.11074 (3)	0.024 (7)	+0.28
H*w*21	−0.34677 (4)	0.21581 (3)	−0.41107 (3)	0.031 (8)	+0.12
H*w*22	−0.44338 (3)	0.27255 (4)	−0.51934 (3)	0.031 (8)	+0.12

neutralized by these strong hydrogen bonds and the expected positive valley of potential occurs. It must be noted that the valley between O32 and HO5 is not well defined in Fig. 4(*b*), because HO5 is 0.84 Å below the plane.

The dipole moments of the molecules were calculated using the monopole and dipole parameters (refinement D), as described by Espinosa *et al.* (1996). They reach 120 (13) C m for YGG and 87 (13) C m for GD. The orientations of these molecular dipole moments are shown in Fig. 1 and are almost in the direction of the line joining the COO^- group to the NH_3^+ group. The dipole moments of the water molecules (5.8 C m for YGG, 5.6 and 4.6 C m for GD) are almost equal within standard uncertainties (approximately one-dimensional) and in the range of those determined for other compounds (3.9–8.9 C m; Spackman, 1992; Dyke & Muenter, 1973). These values are smaller than those obtained by Bouhmaida *et al.* (1999) from a fit of the experimental potential by electric moments (Buckingham, 1959) up to third order (octopolar moments), but in this latter case dipolar moments are only one term of the electrostatic potential expansion.

3.3. Topological analysis of peptide bonds

Topological analysis of the electron density of YGG and GD was performed using Newprop (Souhassou & Blessing, 1999). Analysis of the topological features of hydrogen bonds are published elsewhere (Espinosa, Lecomte & Molins, 1999; Espinosa *et al.*, 1998; Espinosa, Souhassou *et al.*, 1999) as well as the features of C—O covalent bonds (Benabicha *et al.*, 2000). Then, this study will concentrate on the electron-density topology of the peptide unit. All gradient paths and Laplacian maps of the total electron density in the CO—NH planes are similar. As an example, Fig. 5 gives the gradient paths and Laplacian maps in the C1—O1—N2 plane of YGG. The Laplacian maps reveal the shell structure of the atoms; the K-shell of N, C and O atoms is shown by only one contour (the Laplacian values greater than 90 e $Å^{-5}$ are not drawn). Their L-valence shell has local minima which reflect the charge concentration. The three minima around the C1 atom and around the N2 atom are the signatures of the three covalent bonds. Around the O1 atom, one of the three minima is in the direction of the C1—O1 covalent bond. The two other minima of the O1 atom represent the electron density of the lone pairs. Fig. 5(*a*) also gives the position of the critical points (where the gradient of the density vanishes). (3,−3) critical points are found on atomic positions, while (3,−1) critical points are

present in covalent bonds, as expected (Bader, 1990). The gradient vector field displayed in Fig. 5(*b*) in the peptide plane reveals the typical feature of interatomic surfaces: the set of gradient vectors which end at the nuclear position define an atomic basin in which the density can be integrated to obtain the net charges and other moments (Bader, 1990; Souhassou & Blessing, 1999).

As no comparative description of the topological properties of the (3,−1) bond critical point of linear peptide links exists in the literature, the topological properties of the C—Cα, Cα—N, C—N and C═O bonds calculated from X-X electron density studies on five peptide molecules (triglycine: Pichon-Pesme & Lecomte, 1998; Leu-enkephaline: Wiest *et al.*, 1994; *N*-acetyl-L-tryptophane: Souhassou *et al.*, 1991; *N*-acetyl-$\alpha\beta$-

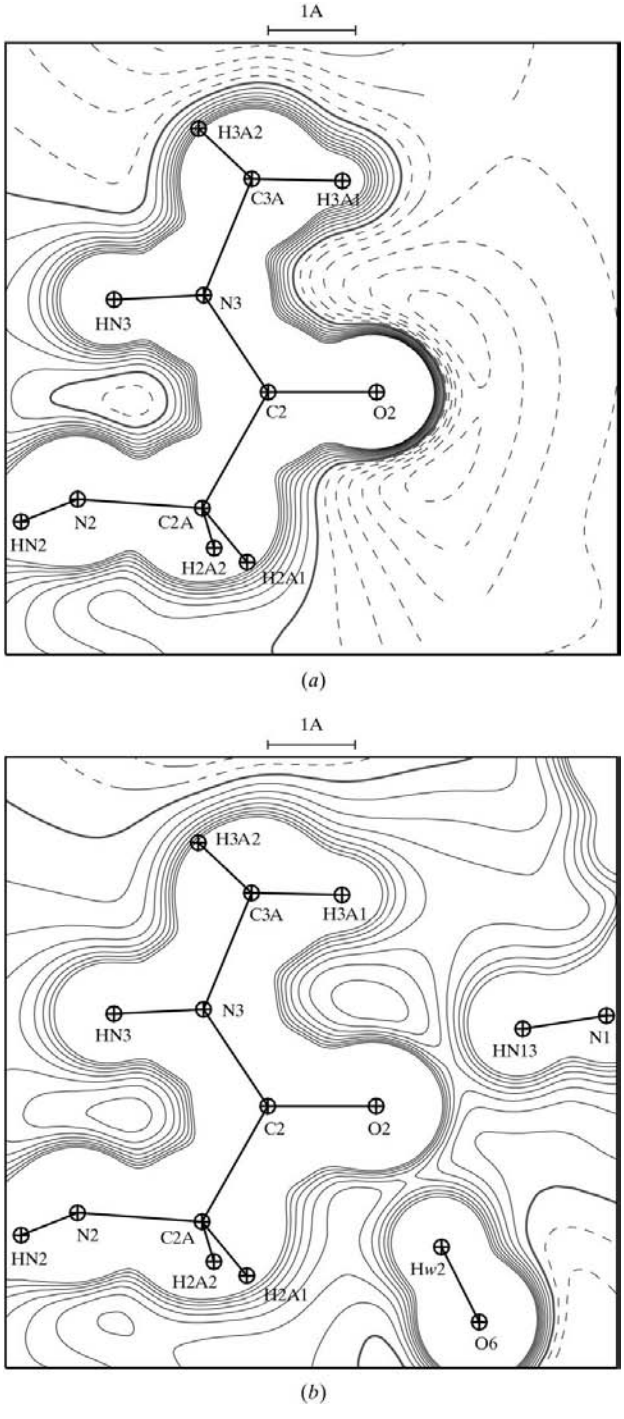

Figure 3
Electrostatic potential in the peptide bond plane generated (*a*) by one YGG molecule and (*b*) by a cluster of two YGG molecules and one water molecule. Contour interval 0.05 e Å^{-1}; positive solid line, negative dashed line, zero heavy line.

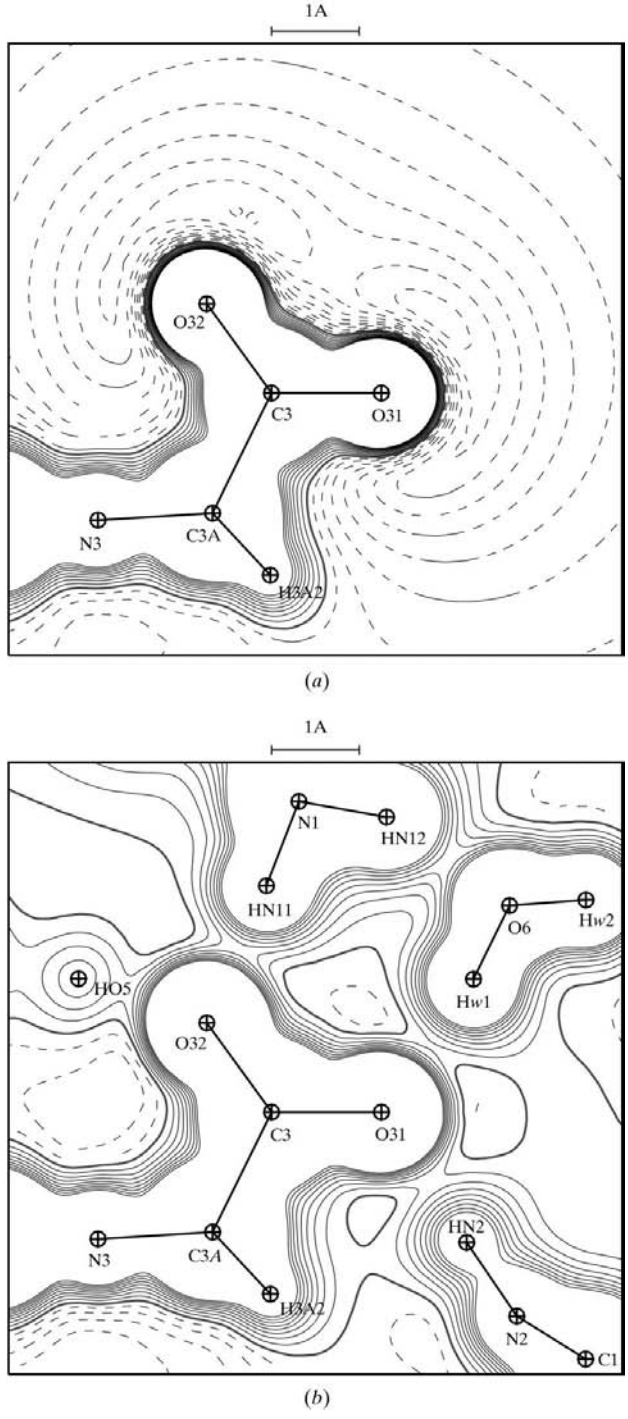

Figure 4
Electrostatic potential in the plane of the carboxyl group generated (*a*) by one YGG molecule and (*b*) by a cluster of two YGG molecules and one water molecule. Contours as in Fig. 3.

Table 3
Bond distances (Å) and angles (°).

(*a*) YGG			
N1—C1A	1.4851 (9)	C2A—C2	1.5233 (9)
C1A—C1B	1.5409 (9)	C2—O2	1.2416 (8)
C1B—C1G	1.5115 (10)	C2—N3	1.3322 (9)
C1G—C1D1	1.3967 (10)	N3—C3A	1.4436 (9)
C1G—C1D2	1.4002 (9)	C3A—C3	1.5307 (10)
C1D1—C1E1	1.3945 (10)	C3—O31	1.2539 (9)
C1D2—C1E2	1.3929 (10)	C3—O32	1.2603 (9)
C1E1—C1Z	1.3904 (10)	O6—H*w*1	0.9640 (5)
C1E2—C1Z	1.3949 (10)	O6—H*w*2	0.9632 (5)
C1Z—OH1	1.3701 (9)	OH1—HO5†	0.9633 (6)
C1A—C1	1.5280 (9)	N1—HN11†	1.0334 (6)
C1—O1	1.2225 (9)	N1—HN12†	1.0324 (6)
C1—N2	1.3491 (9)	N1—HN13†	1.0300 (6)
N2—C2A	1.4492 (8)		
N1—C1A—C1	107.41 (5)	C3A—C3—O32	117.97 (6)
N1—C1A—C1B	111.30 (6)	O31—C3—O32	125.88 (7)
C1A—C1—O1	121.33 (6)	C1A—C1B—C1G	114.77 (6)
C1A—C1—N2	115.17 (6)	C1B—C1G—C1D1	121.49 (6)
O1—C1—N2	123.48 (6)	C1B—C1G—C1D2	120.57 (6)
C1—N2—C2A	119.06 (6)	C1G—C1D1—C1E1	121.54 (6)
C1—C1A—C1B	110.91 (6)	C1G—C1D2—C1E2	121.25 (7)
N2—C2A—C2	115.05 (6)	C1D1—C1E1—C1Z	119.44 (7)
C2A—C2—O2	119.58 (6)	C1D2—C1E2—C1Z	119.62 (7)
C2A—C2—N3	116.95 (6)	C1E1—C1Z—C1E2	120.20 (7)
O2—C2—N3	123.46 (7)	C1E1—C1Z—OH1	121.63 (6)
C2—N3—C3A	124.02 (6)	C1E2—C1Z—OH1	118.16 (6)
N3—C3A—C3	115.02 (6)	H*w*1—O6—H*w*2†	110.00 (5)
C3A—C3—O31	116.05 (6)		
(*b*) For GD			
N1—C1A	1.4705 (7)	C2B—C2G	1.5069 (7)
C1A—C1	1.5219 (7)	C2G—O2D1	1.2159 (6)
C1—O1	1.2327 (6)	C2G—O2D2	1.3168 (7)
C1—N2	1.3373 (7)	O2D2—HD22	0.9604 (4)
N2—C2A	1.4520 (7)	O*w*1—H*w*11†	0.9647 (4)
C2A—C2	1.5346 (7)	O*w*1—H*w*12†	0.9612 (4)
C2—O21	1.2576 (6)	O*w*2—H*w*21†	0.9625 (5)
C2—O22	1.2567 (6)	O*w*2—H*w*22†	0.9713 (5)
C2A—C2B	1.5367 (7)		
N1—C1A—C1	109.53 (4)	O21—C2—O22	124.91 (5)
C1A—C1—O1	121.61 (5)	C2A—C2B—C2G	110.12 (4)
C1A—C1—N2	114.13 (4)	C2B—C2G—O2D1	122.27 (5)
O1—C1—N2	124.26 (5)	C2B—C2G—O2D2	114.15 (4)
C1—N2—C2A	122.25 (4)	O2D1—C2G—O2D2	123.58 (5)
N2—C2A—C2	110.17 (4)	C2G—O2D2—HD22	110.11 (4)
N2—C2A—C2B	110.23 (4)	H*w*11—O*w*1—H*w*12†	108.10 (4)
C2A—C2—O21	118.07 (4)	H*w*21—O*w*2—H*w*22†	111.43 (5)
C2A—C2—O22	117.02 (4)		

† Standard uncertainties calculated from the non-H atoms only.

Table 4
Hydrogen-bonding geometry (Å, °).

D—H···*A*	H···*A*	*D*···*A*	*D*—H···*A*
(*a*) YGG			
O6—H*w*2···O2	1.79	2.7525 (7)	175.7
N1—HN13···O2^{i}	1.92	2.9057 (7)	158.8
N2—HN2···O31^{ii}	1.84	2.8652 (8)	174.2
O6—H*w*1···O31^{iii}	1.85	2.8000 (7)	166.7
OH1—HO5···O32^{iv}	1.7	2.6547 (9)	167.8
N1—HN11···O32^{v}	1.72	2.7453 (9)	172.1
N3—HN3···OH1^{vi}	2	2.8534 (8)	138.7
N1—HN12···O6^{iv}	1.77	2.6898 (9)	145.9
(*b*) GD			
O*w*1—H*w*11···O21	1.73	2.6905 (6)	172.2
N1—HN13···O21^{vii}	1.86	2.8852 (7)	169.9
OD22—HD22···O22^{viii}	1.64	2.5826 (6)	166.9
O*w*1—H*w*12···O22^{ix}	1.77	2.6960 (6)	161.8
N2—HN2···O1^{x}	1.97	2.9875 (6)	167.2
O*w*2—H*w*22···O*w*1^{xi}	1.81	2.7666 (7)	171.6
N1—HN11···O*w*1^{xii}	1.87	2.8110 (7)	149.5
N1—HN12···O*w*2^{xiii}	1.83	2.7595 (7)	147.3
O*w*2—H*w*21···O21^{vii}	1.96	2.9100 (7)	166.3

Symmetry codes: (i) $\frac{1}{2}-x, 1-y, z-\frac{1}{2}$; (ii) $x-\frac{1}{2}, \frac{3}{2}-y, -z$; (iii) $x, y-1, z$; (iv) $\frac{1}{2}+x, \frac{1}{2}-y, -z$; (v) $\frac{1}{2}+x, \frac{3}{2}-y, -z$; (vi) $x, 1+y, z$; (vii) $-1-x, \frac{1}{2}+y, -\frac{1}{2}-z$; (viii) $\frac{1}{2}+x, -\frac{1}{2}-y, -1-z$; (ix) $2-x, y-\frac{1}{2}, -\frac{1}{2}-z$; (x) $-1-x, y-\frac{1}{2}, -\frac{1}{2}-z$; (xi) $\frac{5}{2}-x, -y, z-\frac{1}{2}$; (xiii) $\frac{1}{2}+x, -\frac{1}{2}-y, -z$; (xiii) $-\frac{1}{2}-x, -y, \frac{1}{2}+z$.

dehydrophenylalanine methylamide: Souhassou *et al.*, 1992; *N*-acetyl-L-tyrosine ethyl ester monohydrate: Dahaoui *et al.*, 1999; glycyl-L-threonine dihydrate: Benabicha *et al.*, 2000; GD and YGG, this study) are given in Table 5. The atom names listed in Table 5 are those given in the referenced papers. For each bond, we have calculated the mean and root mean-square deviation (r.m.s.d.) values of each topological parameter, compared with the corresponding value obtained in the promolecule.

For a given bond, we note good agreement between the experimental d_1, d_2 and ρ_{cp} values, their average values being statistically significant [entries (*b*) of Table 5]. It is not generally the case for the ellipticity parameters for which some r.m.s.d. values are very high compared with the average value. Therefore, owing to the poor precision obtained, the experimental ellipticity should not be used to characterize the bond. The relative dispersion of the Laplacian in the Cα—N bonds is due to a large dispersion of the κ' contraction–dilation parameters [κ' = 1.21–0.82; equation (1)] of the non-spherical electron density. We had already observed such a dispersion in this second derivative calculation: in ammonium dihydrogen phosphate (ADP), whose accurate experimental electron density was studied in the paraelectric phase, a linear correlation between the experimental Laplacian and κ' parameters was shown by Pérès *et al.* (1999).

For all the bonds studied, the position of the critical point was determined very precisely (in the range 0.02–0.04 Å) and exactly on the straight line between the two atoms [the sum (d_1 + d_2) equals the interatomic distance]. In the C—Cα bond, the critical point is almost in the middle of the bond, which is slightly closer to the C atom for which the expansion of the valence density [given by the smallest value of κ' in equation (1)] is more important. The CP in the heteronuclear C═O, C—N and Cα—N bonds is always located closer to the less electronegative atom (C) [d_1 = 0.47 (2) Å for C═O, 0.54 (2) Å for C—N and 0.62 (2) Å C for α—N, compared with $\sim$ 0.8 Å for d_2]. The experimental values of the density at the critical point (ρ_{cp}) and of the corresponding Laplacian for the four bonds are typical of shared interactions with an accumulation of electrons along the bond. The shorter the bond, the shorter the distance, the higher the density and correspondingly the higher the experimental average negative Laplacian. This is in agreement with the strength of the bond (C═O, C—N, C—Cα), where the delocalization of the electron is effective. For the sake of comparison, topological properties of a peptide link were also calculated from the superposition of spherical

Table 5
Topological characterization of the electron density of the C—Cα, C═O, C—N, Cα—N peptide bonds.

Bond distances (d), distances (d_1,d_2) from the critical point to each atom, electron density (ρ_{cp}), Laplacian ($\nabla^2\rho$) and ellipticity (ε) values at the critical point. The average standard uncertainties of the position of the critical point and the density at this critical point are estimated to be 10^{-2} Å, 0.05 e Å^{-3}, respectively. We estimate the standard uncertainty on the second derivatives of electron density (ρ,λ) to be 10% of their values (see Espinosa, Souhassou *et al.*, 1999).

(*a*) Experimental data; (*b*) average and r.m.s.d. values. The r.m.s.d. values are calculated as r.m.s.d. = $[\Sigma(x_i - x_m)^2/(n-1)]^{1/2}$. (*c*)–(*e*) Same parameters obtained (*c*) from the promolecule, (*d*) from our database (Pichon-Pesme *et al.*., 1995) and (*e*) from a theoretical calculation (Chang & Bader, 1992). GD = Gly-Asp (this study); YGG = Tyr-Gly-Gly (this study); Trig = triglycine (Pichon-Pesme & Lecomte, 1998); Enk = Leu-enkephalin (Wiest *et al.*, 1994); AcTr = *N*-acetyl-L-tryptophane (Souhassou *et al.*, 1991); AcΔ = *N*-acetyl-αβ-dehydrophenylalanine methylamide (Souhassou *et al.*, 1992); AcTyr = *N*-acetyl-L-tyrosine ethyl ester monohydrate (Dahaoui *et al.*, 1999); GT = glycyl-L-threonine dihydrate (Benabicha *et al.*, 2000).

			d	d_1	d_2	ρ_{cp}	$\nabla^2\rho$	ε
	C—Cα							
(*a*)	GD	C1—C1A	1.522	0.76	0.77	1.77	−13.8	0.21
	YGG	C1—C1A	1.528	0.75	0.78	1.71	−12.8	0.02
	YGG	C2—C2A	1.523	0.74	0.79	1.70	−11.6	0.10
	Trig	C11—C1A1	1.522	0.80	0.72	1.63	−11.6	0.18
	Trig	C12—C1A2	1.519	0.81	0.71	1.69	−11.8	0.20
	Trig	C21—C2A1	1.512	0.76	0.75	1.77	−14.0	0.14
	Trig	C22—C2A2	1.516	0.79	0.73	1.67	−11.1	0.28
	Enk	C9—C1	1.524	0.70	0.82	1.68	−13.8	0.11
	Enk	C11—C10	1.522	0.71	0.82	1.65	−12.8	0.10
	Enk	C13—C12	1.517	0.71	0.81	1.66	−13.0	0.13
	Enk	C22—C14	1.532	0.73	0.80	1.61	−12.0	0.18
	AcTr	C2—C1	1.500	0.78	0.71	1.70	−12.2	0.07
	AcTr	C4—C3	1.541	0.79	0.75	1.73	−12.8	0.14
	AcΔ	C2—C1	1.504	0.78	0.73	1.71	−13.2	0.11
	AcΔ	C11—C3	1.503	0.76	0.75	1.80	−12.9	0.13
	AcTyr	C—C1	1.507	0.80	0.71	1.67	−12.0	0.10
	GT	C1—C1A	1.516	0.77	0.74	1.74	−14.4	–
(*b*)	Average value		1.518	0.76	0.76	1.70	−12.7	0.14
	R.m.s.d.		0.011	0.03	0.04	0.05	0.9	0.06
(*c*)	Promolecule		1.524	0.76	0.76	1.15	1.4	0.02
(*d*)	Amino acid database		1.524	0.78	0.75	1.76	−14.4	0.12
(*e*)	Theoretical calculation		1.509	0.72	0.79	1.88	−20.5	0.09
	Cα—N							
(*a*)	GD	C2A—N2	1.452	0.60	0.85	1.80	−8.7	0.08
	YGG	C2A—N2	1.449	0.64	0.81	1.79	−8.8	0.10
	YGG	C3A—N3	1.444	0.58	0.86	1.69	−7.0	0.11
	Trig	C1A2—N12	1.447	0.61	0.84	1.80	−12.5	0.07
	Trig	C1A3—N13	1.451	0.60	0.85	1.79	−12.3	0.16
	Trig	C2A2—N22	1.443	0.58	0.87	1.74	−12.1	0.17
	Trig	C2A3—N23	1.446	0.62	0.83	1.79	−11.7	0.10
	Enk	C10—N2	1.457	0.66	0.80	1.78	−9.1	0.09
	Enk	C14—N4	1.456	0.64	0.82	1.81	−10.9	0.05
	Enk	C23—N5	1.459	0.65	0.81	1.76	−8.8	0.07
	AcTr	C3—N1	1.448	0.61	0.84	1.89	−9.6	0.09
	AcTr	C5—N2	1.450	0.61	0.84	1.82	−9.3	0.09
	AcD	C3—N1	1.412	0.61	0.81	1.93	−12.0	0.12
	AcD	C12—N2	1.448	0.63	0.82	1.90	−14.4	0.08
	AcTyr	CA—N	1.451	0.62	0.83	1.77	−9.9	0.07
	GT	C2A—N2	1.447	0.61	0.84	1.70	−5.6	–
(*b*)	Average value		1.447	0.62	0.83	1.8	−10.2	0.10
	R.m.s.d.		0.011	0.02	0.02	0.1	2.3	0.03
(*c*)	Promolecule		1.457	0.66	0.80	1.40	3.0	0.01
(*d*)	Amino acid database		1.457	0.63	0.82	1.92	−13.2	0.11
(*e*)	Theoretical calculation		1.438	0.49	0.95	1.88	−19.4	0.05
	C—N							
(*a*)	GD	C1—N2	1.337	0.54	0.80	2.25	−20.1	0.30
	YGG	C1—N2	1.349	0.56	0.79	2.31	−21.4	0.13
	YGG	C2—N3	1.332	0.55	0.78	2.42	−22.6	0.16
	Trig	C11—N12	1.333	0.52	0.81	2.32	−23.4	0.28
	Trig	C12—N13	1.335	0.56	0.78	2.40	−26.2	0.33
	Trig	C21—N22	1.335	0.55	0.79	2.40	−25.4	0.27
	Trig	C22—N23	1.339	0.57	0.77	2.37	−24.6	0.28
	Enk	C9—N2	1.333	0.54	0.80	2.46	−27.9	0.22
	Enk	C11—N3	1.341	0.54	0.80	2.43	−27.2	0.23
	Enk	C13—N4	1.339	0.54	0.80	2.44	−27.5	0.22
	Enk	C22—N5	1.336	0.54	0.80	2.45	−27.7	0.22
	AcTr	C2—N1	1.334	0.52	0.81	2.37	−20.0	0.07
	AcTr	C4—N2	1.338	0.53	0.81	2.36	−19.9	0.08
	AcΔ	C2—N1	1.347	0.56	0.79	2.29	−17.2	0.26
	AcΔ	C11—N2	1.336	0.57	0.76	2.40	−21.0	0.20
	AcTyr	C—N	1.345	0.54	0.80	2.30	−23.2	0.18
	GT	C1—N2	1.339	0.56	0.78	2.39	−22.4	–
(*b*)	Average value		1.338	0.55	0.79	2.4	−23.4	0.21
	R.m.s.d.		0.005	0.01	0.01	0.1	3.2	0.08
(*c*)	Promolecule		1.337	0.57	0.76	1.72	−0.5	0.03
(*d*)	Amino acid database		1.337	0.54	0.79	2.43	−28.6	0.24
(e)	Theoretical calculation		1.346	0.44	0.90	2.26	−15.0	0.02
	C═O							
(*a*)	GD	C1—O1	1.233	0.46	0.77	2.59	−16.1	0.09
	YGG	C1—O1	1.223	0.45	0.77	2.79	−17.9	0.10
	YGG	C2—O2	1.242	0.48	0.77	2.71	−22.6	0.07
	Trig	C11—O11	1.235	0.51	0.73	2.78	−26.7	0.11
	Trig	C12—O12	1.238	0.49	0.75	2.80	−28.8	0.19
	Trig	C21—O21	1.235	0.49	0.75	2.73	−26.1	0.21
	Trig	C22—O22	1.235	0.49	0.75	2.80	−29.1	0.18
	Enk	C9—O2	1.241	0.46	0.78	2.92	−31.8	0.07
	Enk	C11—O3	1.240	0.46	0.78	2.92	−31.8	0.07
	Enk	C13—O4	1.242	0.46	0.78	2.91	−31.9	0.07
	Enk	C22—O5	1.235	0.46	0.78	2.94	−31.4	0.07
	AcTr	C2—O1	1.248	0.50	0.75	2.74	−21.2	0.09
	AcTr	C4—O2	1.232	0.49	0.75	2.81	−21.0	0.09
	AcΔ	C2—O1	1.238	0.50	0.74	2.86	−23.7	0.04
	AcΔ	C11—O2	1.239	0.49	0.75	2.96	−26.5	0.12
	AcTyr	C—O	1.225	0.49	0.76	2.88	−29.4	0.10
	GT	C1—O1	1.232	0.49	0.74	2.75	−28.0	–
(*b*)	Average value		1.236	0.48	0.76	2.8	−26.1	0.10
	R.m.s.d.		0.005	0.02	0.02	0.1	3.8	0.05
(*c*)	Promolecule		1.240	0.47	0.77	2.08	4.6	0.02
(*d*)	Amino acid database		1.240	0.52	0.72	2.89	−31.3	0.14
(*e*)	Theoretical calculation		1.227	0.40	0.82	2.75	4.7	0.06

atomic densities (promolecule) and from the static electron density calculated from our amino acid electron density database (Pichon-Pesme *et al.*, 1995). The critical point position remains constant whatever the charge density model: the bonding interaction then has no significant effect on the position of the critical point within the experimental accuracy. However, as expected, the promolecule density is smaller and the Laplacian has an opposite sign ($\nabla^2\rho > 0$, except for the very small value of the C—N Laplacian). In the promolecule model, the density in the bond is only the sum of the spherical densities of two atoms and no electron rearrangement can occur. The absolute value of the Laplacian and the density at CP calculated with the amino acid electron-density database (Pichon-Pesme *et al.*, 1995) are greater than those obtained by averaging on the peptide link [Table 5, entry (*d*)]. This observation is in line with our results on crambin (Jelsch *et al.*, 2000). Indeed, the P_{lm} parameters of the database give an overestimation of static density. Further work is therefore needed to extract better average charge-density parameters to fill up the experimental database. The values derived from the

triple zeta calculation of Chang & Bader (1992), see Table 5, entry (*e*), are generally different from our average experimental topological parameters, except for ρ_{cp}, which agrees within 10% with the experiment: all positions of the critical points differ from those derived from experimental data (0.13 Å in the C—N bond, for example). We cannot make any comparison between parameters calculated at critical point positions, because their positions obtained from theory are different from those given in this experimental study and therefore even the agreement for ρ_{cp} may be accidental. More accurate calculations and also more precise estimation of κ' (Pérès *et al.*, 1999) is needed in order to really be able to compare these quantities. Restricted kappa refinement based on theoretical calculations as proposed by Abramov *et al.* (1999) could be necessary to classify all these bonds lengths in terms of electron density topology.

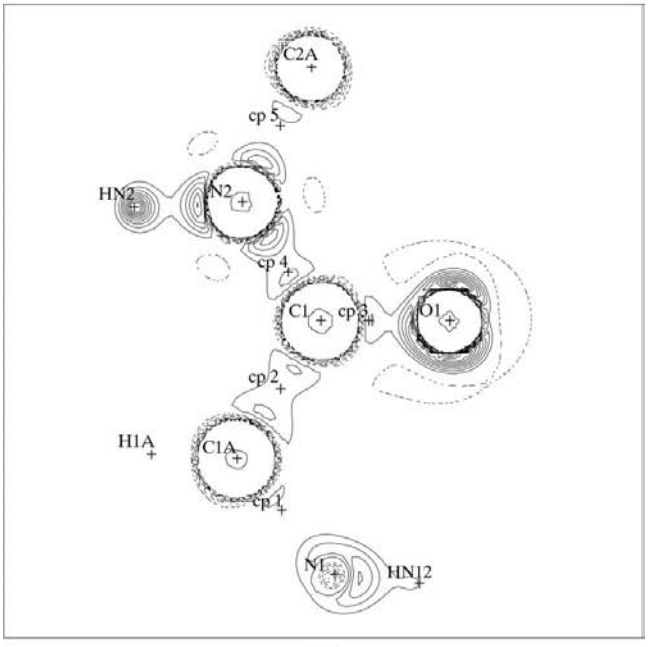

(*a*)

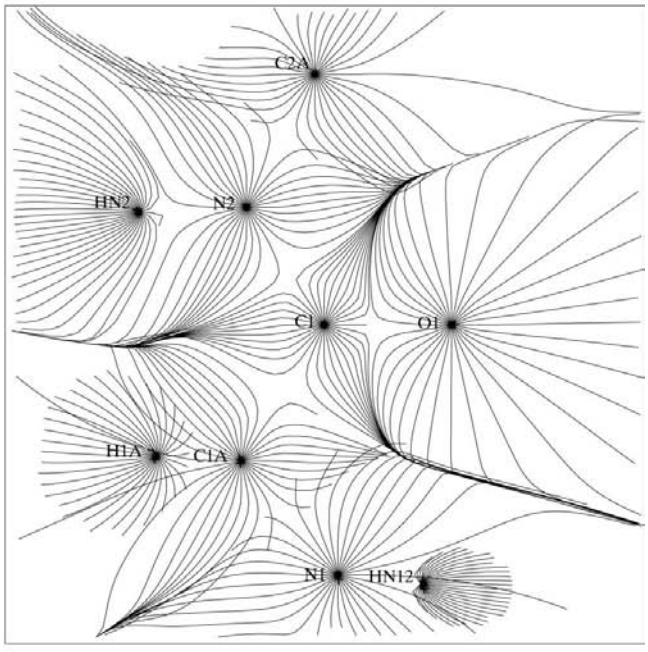

(*b*)

Figure 5
Laplacian of the electron density, (*a*) (3,−1) critical points (cp) and (*b*) gradient paths in the YGG peptide bond plane. Contour intervals for the Laplacian are 10 e Å^{-5}; positive dashed line, negative solid line, zero contour omitted.

References

Abramov, Yu. A., Volkov, A. V. & Coppens, P. (1999). *Chem. Phys. Lett.* pp. 81–86.
Allen, F. (1986). *Acta Cryst.* B**42**, 515–522.
Bader, R. F. W. (1990). *Atoms in Molecules, a Quantum Theory*. Oxford Science Publications.
Benabicha, F., Pichon-Pesme, V., Jelsch, C., Lecomte, C. & Khmou, A. (2000). *Acta Cryst.* B**56**, 155–165.
Blessing, R. H. (1987). *Crystallogr. Rev.* **1**, 3–58.
Blessing, R. H. (1989). *J. Appl. Cryst.* **22**, 396–397.
Bouhmaida, N., Ghermani, N.-E., Lecomte, C. & Thalal, A. (1999). *Acta Cryst.* A**55**, 729–738.
Buckingham, A. D. (1959). *Q. Rev. Chem.* **13**, 183–241.
Burnett, M. N. & Johnson, C. K. (1996). *ORTEP*III. Report ORNL-6895. Oak Ridge National Laboratory, Tennessee, USA.
Carson, W. M. & Hackert, M. L. (1978). *Acta Cryst.* B**34**, 1275–1280.
Chang, C. & Bader, R. F. W. (1992). *J. Phys. Chem.* **96**, 1654–1662.
Chen, L. & Craven, B. M. (1995). *Acta Cryst.* B**51**, 1081–1097.
Clementi, E. & Raimondi, D. L. (1963). *J. Chem. Phys.* **41**, 2686–2689.
Coppens, P., Guru Row, T. N., Leung, P., Stevens, E. D., Becker, P. J. & Yang, Y. W. (1979). *Acta Cryst.* A**35**, 63–72.
Cromer, D. T. (1974). *International Tables for X-ray Crystallography*, edited by J. A. Ibers and W. E. Hamilton, pp. 148–151. Birmingham: Kynoch Press. (Present distributor Kluwer Academic Publishers, Dordrecht.)
Dahaoui, S., Jelsch, C., Howard, J. A. K. & Lecomte, C. (1999). *Acta Cryst.* B**55**, 226–230.
Dyke, T. R. & Muenter, J. S. (1973). *J. Chem. Phys.* **59**, 3125–3127.
Eggleston, D. S. & Hodgson, D. J. (1982). *Int. J. Peptide Protein Res.* **19**, 206–211.
Espinosa, E., Lecomte, C. & Molins, E. (1999). *Chem. Phys. Lett.* **300**, 745–748.
Espinosa, E., Lecomte, C., Molins, E., Veintemillas, S., Couson, A. & Paulus, W. (1996). *Acta Cryst.* B**52**, 519–534.
Espinosa, E., Molins, E. & Lecomte, C. (1998). *Chem. Phys. Lett.* **285**, 170–173.
Espinosa, E., Souhassou, M., Lecomte, C. & Lachekar, H. (1999). *Acta Cryst.* B**55**, 563–572.
Ghermani, N.-E., Bouhmaida, N. & Lecomte, C. (1992). *ELECTROS.* Internal Report URA CNRS 809, University of Nancy 1, France.
Hansen, N. K. & Coppens, P. (1978). *Acta Cryst.* A**34**, 909–921.
Jelsch, C., Pichon-Pesme, V., Lecomte, C. & Aubry, A. (1998). *Acta Cryst.* D**54**, 1306–1318.
Jelsch, C., Teeter, M. M., Lamzin, V., Pichon-Pesme, V., Blessing, R. H. & Lecomte, C. (2000). *Proc. Natl Acad. Sci USA*, **97**, 3171–3176.
Lecomte, C., Ghermani, N. E., Pichon-Pesme, V. & Souhassou, M. (1992). *J. Mol. Struct. (Theochem.)* **255**, 241–260.
McCandlisch, L. E., Stout, G. H. & Andrews, L. S. (1975). *Acta Cryst.* A**31**, 245–249.
Pérès, N., Boukhris, A., Souhassou, M., Gavoille, G. & Lecomte, C. (1999). *Acta Cryst.* A**55**, 1038–1048.
Pichon-Pesme, V. & Lecomte, C. (1998). *Acta Cryst.* B**54**, 485–493.

Pichon-Pesme, V., Lecomte, C. & Lachekar, H. (1995). *J. Phys. Chem.* **99**, 6242–6250.
Pichon-Pesme, V., Lecomte, C., Wiest, R. & Bénard, M. (1992). *J. Am. Chem. Soc.* **114**, 2713–2715.
Sheldrick, G. M. (1990). *Acta Cryst.* A**46**, 467–473.
Souhassou, M. & Blessing, R. H. (1999). *J. Appl. Cryst.* **32**, 210–217.
Souhassou, M., Lecomte, C., Blessing, R. H., Aubry, A., Rohmer, M.-M., Wiest, R. & Bénard, M. (1991). *Acta Cryst.* B**47**, 253–266.
Souhassou, M., Lecomte, C., Ghermani, N.-E., Rohmer, M.-M., Wiest, R., Bénard, M. & Blessing, R. H. (1992). *J. Am. Chem. Soc.* **114**, 2371–2382.
Spackman, M. A. (1992). *Chem. Rev.* **92**, 1769–1797.
Stewart, R. F., Davidson, E. R. & Simpson, W. T. (1965). *J. Chem. Phys.* **43**, 175–187.
Wiest, R., Pichon-Pesme, V., Bénard, M. & Lecomte, C. (1994). *J. Phys. Chem.* **98**, 1351–1362.